

Comments on theory of volume reflection and radiation in bent crystals

M. V. BONDARENCO

Kharkov Institute of Physics & Technology, 1 Academic Str., Kharkov 61108, Ukraine

Summary. — Recent theoretical results on charged particle interaction with planar oriented thin bent crystals are reviewed, with the emphasis on dynamics in the continuous potential. Influence of boundary conditions on the volume-reflected beam profile is discussed. Basic properties of coherent bremsstrahlung in a bent crystal are highlighted.

PACS 61.85.+p – bent crystal; volume reflection; coherent bremsstrahlung.

1. – Introduction

Passage of charged particles through a bent crystal, even in a planar orientation, is a complex phenomenon, theoretical treatment of which used to rely on computer simulation. However, sometimes complexity begets simplicity, which may permit analytic advances – like it was commonly practiced before the advent of computers. Actually, computer and analytic calculations complement one another: analytic formulas provide general understanding of the phenomenon, and may serve for experiment planning, while computer can offer precise predictions for an established experimental setting.

An example of a problem where analytic approach did bring fruit is fast charged particle passage through a planar oriented uniformly bent crystal. Even though the planar orientation and uniformity of the bending enormously simplify the dynamics, reducing it to radial 1d, yet there are impediments for solution of the whole beam-crystal interaction problem: how to analytically describe particle passage through many inter-planar intervals, and how to analytically average over the initial particle impact parameters. Alleviation came from the use of a simplified (parabolic) model for inter-planar continuous potential, which made analytic solution for single volume reflection (VR) feasible [1]. It appears that precise inter-planar potential shape is of minor consequence anyway, and the piecewise harmonic potential model yields fair agreement with the experiment.

A different story is the bremsstrahlung emitted by the fast particle in a bent crystal. There, a large contribution comes from the dipole coherent bremsstrahlung, which can be described for an arbitrary inter-planar potential. Analytic theory of dipole coherent radiation in bent crystals (CBBC) was constructed in [2].

The present short note surveys the physical picture of volume reflection and radiation in a bent crystal, in the pure continuous potential.

2. – Volume reflection

2.1. Essence of the effect. – VR effect manifests itself in the same region of E/R ratio as channeling, with the proviso that the particle entrance angle with respect to active crystallographic planes must be well above critical. However, the correlation between the particle deflection angle and the crystal curvature for VR appears to be more intricate than that for channeling:

1. in VR particles deflect to the side opposite to that of the crystal bending;
2. the deflection angle tends to a finite limit with the increase of R/R_c ratio, although $R = \infty$ corresponds to a straight crystal and no net deflection; this limiting value is of the order of critical angle θ_c both for positive and for negative particles, though with different numerical coefficients.

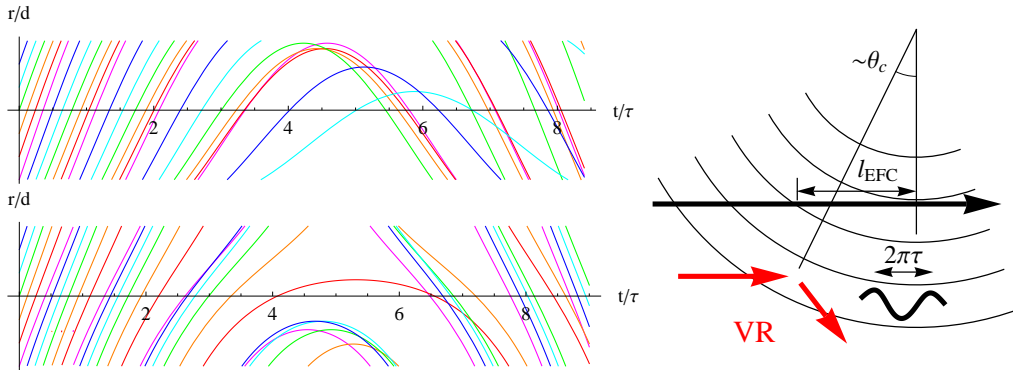


Fig. 1. – Left-side frame – trajectory filling of an exemplary inter-planar interval by an initially transversely uniform particle beam (top – positive particles, bottom – negative particles). The deficit of positively directed force in VR area causes the negative net deflection of the beam. Right-side frame – comparison of ultra-high energy ($R \ll 4R_c$, $l_{EFC} \ll 2\pi\tau$) with moderately high energy ($R \gg 4R_c$, $2\pi\tau \ll l_{EFC}$) particle passage. In the latter case the particle net deflection angle is non-zero and $\sim \theta_c$, regardless of the particle charge sign.

The qualitative explanation of the opposite deflection direction is given in [3]: “For a small crystal curvature, that is $R \gg R_c$, the turning points of all particles gather in a narrow region near the inner wall of a planar channel. The strong electric field of the crystal plane is directed along R and at the turning points it imparts to the particle an angular deflection towards the opposite direction with respect to the crystal bending, producing volume reflection.” For explanation of feature 2 the latter argument is not sufficient yet. It is known that for negative particles the force in the reflection point is much smaller than for positive ones, but nevertheless, the deflection angle for these cases is of the same order. For a closer look, let us draw a graph of the family of particle trajectories in an exemplary inter-planar interval (Fig. 1). The figure reveals that in inter-planar channels there emerge regions devoid of particles. This entails deficit of force of a definite (positive) sign acting on the beam as a whole; hence, the mean

deflection angle must be negative. At sufficiently large R , the void transverse dimension is $\sim d$, so $F \sim F_{\max}$, and the longitudinal dimension is $\sim \tau = \sqrt{R_c d}/2$ (the channeling oscillation timescale)⁽¹⁾; none of these parameters involve R , therefore, there is a limiting value $\lim_{R \rightarrow \infty} \langle \theta \rangle_b$ independent of R : $\langle \theta \rangle_b \sim \frac{1}{E} F_{\max} \tau = \theta_c$.

Of course, if one overbends the crystal, all the intra-crystal space becomes uniformly covered by the particle flow, then voids and therewith the VR effect disappear. In [1, 2] it was proved that if $E \rightarrow \infty$, i.e., $R/R_c \rightarrow 0$, then $\int db \theta(b) = 0$.

Ex adverso the existence of VR effect can be explained more concisely: When a high-energy particle passes through a bent crystal, after its entrance the angle between its velocity and the active planes decreases. When this angle becomes $\sim \theta_c$, the particle experiences strong influence of the continuous potential field on the length τ . If this length is shorter than $l_{\text{EFC}} = \sqrt{2Rd}$, it would be capable of making the particle channeled. But for motion in a stationary potential, an unbound particle cannot pass into bound state. Hence, at $\pi\tau < l_{\text{EFC}}$, i.e. $R > \frac{\pi^2}{4} R_c$, the particle net inclination angle can not become smaller than θ_c , which implies that the particle will reflect when the angle becomes $\sim \theta_c$ – see right-side frame of Fig. 1.

2.2. Boundary condition sensitivity. – Although the term ‘volume’ reflection signifies that the deflection arises somewhere in the crystal volume, and therefore should not depend on the crystal boundaries, but to some degree, the boundary effects still manifest themselves when investigating the final beam profile detail.

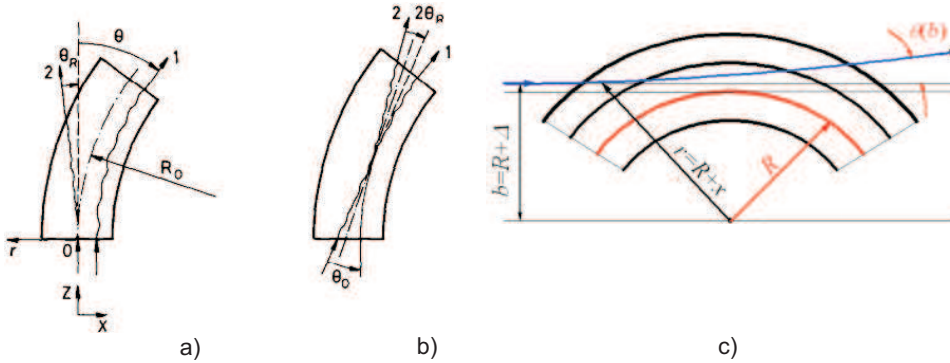


Fig. 2. – Possible boundary conditions for VR in a uniformly bent crystal. Left-side frame, cases a) and b) (the figure is taken from [4]) – particle entrance through a flat front face of a thin bent crystal. At modern practice, the x -dimension of the crystal is actually much wider than its z -dimension. Right-side frame (figure taken from [5]) – particle entrance through the curved lateral surface of a longitudinally extended crystal; this type of boundary conditions is also adopted in [6].

First of all, even for a uniformly bent crystal, there are several options for particle beam entrance to the crystal – see Fig. 2. At practice one usually deals with case b), when the particle entrance angle θ_0 is much greater than critical; the corresponding theory was worked out in [7, 1]. But at channeling experiments, there also arises case a), which

⁽¹⁾ Note that this scale is R/R_c times shorter than scale $R\theta_c$ within which the particle trajectory substantially differs from a straight line. At $R \gg R_c$, in principle one should mind the existence of two longitudinal scales in the volume reflection phenomenon.

was studied in the pioneering work [4]. In the latter case, the particles enter the crystal tangentially to the active planes, so, at $R \gg R_c$ most of the particles are channeled, but a small fraction of particles hitting one-sided vicinity of the top of potential barrier belongs to volume reflection. For the latter fraction, it is supposed that owing to symmetry of the trajectory in a central field with respect to the reflection (minimal-radius) point, the deflection angle θ for case a) is half the value for case b). But yet there is a slight dependence of the deflection angle on the impact parameter, and it is this dependence which determines the final beam shape. So, a question remains, whether the final beam profiles for cases a) and b) are similar.

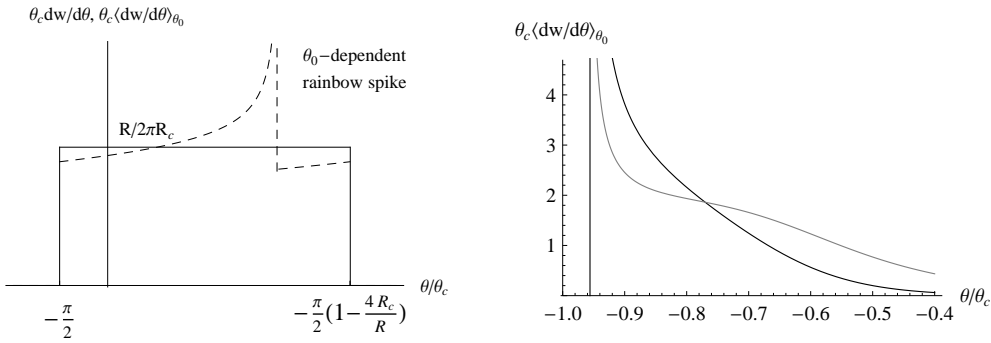


Fig. 3. – Left-side frame – angular distribution in a VR beam for positive particles, at $R > 4R_c$, without account of multiple scattering. Solid curve – distribution averaged over a small variations of initial large angle θ_0 , dashed curve – for a definite θ_0 . Right-side frame – the angular distribution for negative particles, plotted for $R = 25R_c$. Black curve – for boundary condition of type b) (averaged over a small vicinity of large angle θ_0), gray curve – for case a) and stretched in θ by the factor of 2. The peaks on the figures are due to rainbow phenomena[1].

To establish correspondence between the profiles for cases a) and b), neglecting meanwhile the multiple scattering, note that θ depends on the impact parameter b only through the transverse energy $E_{\perp} = E \frac{\theta^2}{2} + V_{\text{eff}}(-b)$, with $V_{\text{eff}}(-b) = V(-b) + \frac{Eb}{R}$, whereas $\theta(E_{\perp})$ is a universal periodic function of E_{\perp} with the period $\Delta E_{\perp} = \frac{Ed}{R} \sim \frac{R_c}{R} V_0 \ll V_0$ [7]. However, dependencies $E_{\perp}(b)$ are different under different boundary conditions. For case b), $\theta(E_{\perp})$ spans many periods as b varies from $-\frac{d}{2}$ to $\frac{d}{2}$, and $E_{\perp}(b)$ dependence, basically, is linear within each period of $\theta(E_{\perp})$. But for case a) $\theta(E_{\perp})$ spans only one period, and the dependence of V_{eff} near its top is essential. Now, for positive particles this behavior is close to linear, too, and so for positive particles boundary conditions a) and b) yield basically isomorphic profiles. On the contrary, for negative particles $V_{\text{eff}}(b)$ behavior near the top is quadratic. Thus, the relation between the profiles appears to be $2\theta^a(\sqrt{\nu}) = \theta^b(\nu)$, where ν is the transverse kinetic energy on the entrance to the reflection inter-planar interval, rescaled to vary from 0 to 1. See Fig. 3, right-side frame. ⁽²⁾

As for boundary condition of type c) (see Fig. 2), which simplifies the theoretical problem by making it entirely centrally-symmetric, it yields $\frac{dw}{d\theta}$ similar to the case b), though indicatrix $\theta(b)$ has a somewhat different double-periodic behavior [5].

⁽²⁾ In paper [1], footnote 14, it is asserted that for case b) there is no rainbow, but more precisely, the rainbow significantly attenuates, though in principle remains.

2.3. Multiple scattering. – Intrinsic VR angular distributions shown in Fig. 3 have an interesting edgy structure, for negative particle case being yet asymmetric and containing a significant rainbow. But at practice, those distinction features will be obscured by multiple scattering. However, the extent of the VR area $2\pi\tau = \pi\sqrt{2?R_c d} \sim 50\mu\text{m}$ is much shorter than the crystal thickness $L \sim 1\text{mm}$. Thereat, the multiple scattering effects accumulate mainly away from the VR point (upstream and downstream of it). This allows one to view the aggregate distribution as a convolution of successive scattering probabilities [7]:

$$(1) \quad \frac{dw_{\text{real}}}{d\theta} \approx \int_{-\infty}^{\infty} d\theta_1 \frac{e^{-(\theta-\theta_1)^2/2\sigma_{\text{am}}^2}}{\sqrt{2\pi}\sigma_{\text{am}}} \frac{dw_{\text{v.r.}}}{d\theta_1} \quad \left(\int_{-\infty}^{\infty} d\theta \frac{dw_{\text{real}}}{d\theta} = \int_{-\infty}^{\infty} d\theta \frac{dw_{\text{v.r.}}}{d\theta} = 1 \right),$$

where $dw_{\text{v.r.}}/d\theta$ is calculated with the neglect of multiple scattering, and σ_{am}^2 is the mean square angle of multiple scattering in an amorphous target of the same thickness. Consideration beyond approximation (1) will be given elsewhere.

In principle, Eq. (1) can be inverted; it is noteworthy that Fourier transforms of $dw_{\text{real}}/d\theta$ and $dw_{\text{v.r.}}/d\theta$ are proportional, and should both have negative regions. But unfortunately, under conditions of binned measurement of $dw_{\text{real}}/d\theta$, only first few moments of the angular distribution can be accessed reliably.

2.4. Moments of the final angular distribution. – The complete analytic calculation of $dw_{\text{v.r.}}/d\theta$ was made within the model of [1]. According to this solution, the limiting value for $\theta_{\text{v.r.}}/\theta_c$ at $R/4R_c \rightarrow \infty$ amounts $\pi/2$ for positively charged particles, and 1 for negatively charged particles. More precisely, this is the outer edge of the angular distribution. The deflection angle mean value involves an $\mathcal{O}(R_c/R)$ correction:

$$(2) \quad \langle \theta \rangle = \int d\theta \theta \frac{dw_{\text{real}}}{d\theta} = \int d\theta \theta \frac{dw_{\text{v.r.}}}{d\theta} = \begin{cases} -\frac{\pi}{2}\theta_c \left(1 - \frac{2R_c}{R}\right) & \text{for pos. charged particles} \\ -\theta_c \left(1 - 1.3\frac{R_c}{R} \ln \frac{R}{R_c}\right) & \text{for neg. charged particles} \end{cases}$$

(the coefficient 1.3 for negative particles needs more precise evaluation). For protons, prediction (2) was compared with experiment in [1], see also Fig. 4 below.

The second moment, mean square deflection, under assumption (1) possesses the property of additivity, even for non-gaussian $dw_{\text{v.r.}}/d\theta$:

$$(3) \quad \sigma_{\text{real}}^2 \approx \int_{-\infty}^{\infty} d\theta (\theta - \langle \theta \rangle)^2 \int_{-\infty}^{\infty} d\alpha \frac{e^{-\frac{(\theta-\alpha)^2}{2\sigma_{\text{am}}^2}}}{\sqrt{2\pi}\sigma_{\text{am}}} \frac{dw_{\text{v.r.}}}{d\alpha} = \sigma_{\text{am}}^2 + \bar{\sigma}_{\text{v.r.}}^2,$$

where $\bar{\sigma}_{\text{v.r.}}^2 = \int_{-\infty}^{\infty} d\theta (\theta - \langle \theta \rangle)^2 \frac{dw_{\text{v.r.}}}{d\theta}$. For positively charged particles, acquiring rectangular intrinsic final angular distribution at $\frac{4R_c}{R} < 1$, evaluation of $\bar{\sigma}_{\text{v.r.}}$ gives

$$(4) \quad \bar{\sigma}_{\text{v.r.}} = \frac{\pi}{\sqrt{3}} \frac{R_c}{R} \theta_c \quad (\text{for positively charged particles}).$$

Experiment [3] used procedure (3), i.e., formula $\bar{\sigma}_{\text{v.r.}} = \sqrt{\sigma_{\text{real}}^2 - \sigma_{\text{am}}^2}$, to determine $\bar{\sigma}_{\text{v.r.}}$. Comparison of experimental data with Eq. (4) is shown in Fig. 4 by dashed line.

For negatively charged particles, where the final profile is skew, its third moment is also non-zero: $\int d\theta (\theta - \langle \theta \rangle)^3 \frac{dw_{\text{real}}}{d\theta} \approx \int d\theta (\theta - \langle \theta \rangle)^3 \frac{dw_{\text{v.r.}}}{d\theta} \neq 0$.

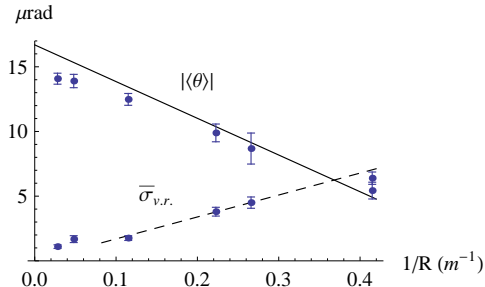


Fig. 4. – Deflection angle mean value (Eq. (2), solid line) and rms deviation (Eq. (4), dashed line) for a parabolic model of inter-planar potential compared with CERN SPS experimental data [3] (protons, $E=400$ GeV).

2.5. Conditions for quality VR deflection. – Joint consideration of beam spread in the continuous potential, multiple scattering in the silicon material, and the initial beam angular divergence has led [1] to a system of conditions needed for practical application of VR to beam steering at accelerators:

$$(5) \quad \frac{L}{1 \text{ mm}} < \frac{E}{100 \text{ GeV}} < \frac{R}{\text{m}}, \left(\frac{20 \mu\text{rad}}{\sigma_0} \right)^2,$$

where σ_0 is the initial beam rms divergence. Conditions (5) are fairly well met in experiments [3].

2.6. VR at $\theta_0 \sim \theta_c$. – The theoretical description of VR in [7, 1] focussed on the case $\theta_0 \gg \theta_c$, when the process may be regarded as independent of the crystal boundaries. But in experiments, VR is often investigated in parallel with channeling, with a continuous passage from one regime to another. In the transition regime, the final beam angular distribution must acquire substantial θ_0 -dependence. Investigation of this dependence is important as well (see [8]).

3. – Radiation in thin uniformly bent crystals

Observation of inelastic processes evoked by a fast particle traveling a bent crystal may be used for extraction of information about particle trajectories at real conditions. Among possible inelastic processes, the coherent radiation in the near-forward direction⁽³⁾ benefits from existence of a local correspondence between the photon ω and the longitudinal coordinate z it is emitted from. This relation is particularly simple (geometric rather than dynamic) at large ω , corresponding to z away from the VR area. There, the particle deflection from the straight line is only perturbative, opposite in sign for electrons and positrons. Here we will confine ourselves to discussion of the latter simplest case – coherent bremsstrahlung in a bent crystal (CBBC).

⁽³⁾ The direct radiation from the fast passing particle is only significant for electrons and positrons, whereas for beam deflection applications the primary interest is on protons. However, ultra-relativistic positrons have essentially the same trajectory as protons of equal energy, so one indirectly can test proton passage through experiments with positrons.

3.1. CBBC intensity as a sum of infinitesimal straight-crystal contributions. – The first, analytic, calculation of coherent bremsstrahlung in a bent crystal was undertaken in [9] (in appendix of a paper primarily dedicated to *channeling* radiation in a uniformly bent crystal). Fourier decomposition of the bent crystal continuous potential yielded Fresnel functions, which describe both volume effects (step-like asymptotics), and the oscillations due to edge effects. But at practice usually the edge effects are negligible, and the Fresnel functions may be replaced by a Heavyside unit-step function, which led to Eq. (A.16) of [9]:

$$(6) \quad d\sigma^B(\omega, \theta_0) = \frac{1}{\Delta\psi(R, L) - \theta_{\min}} \int_{\theta_{\min}}^{\Delta\psi(R, L)} d\sigma^S(\omega, \theta_x; L) d\theta_x,$$

with $d\sigma^S$, $d\sigma^B$ the radiation differential cross-sections in a straight and in a bent crystal, $\Delta\psi$ the angle between the particle velocity and active crystallographic planes on the crystal edge, and $\theta_{\min} \simeq \frac{q_{\min}d}{2\pi} \ll \Delta\psi$. This representation in form of unweighted θ_x -averaging is only valid at $R = \text{const}$. Eq. (6) also assumes symmetric orientation of the beam with respect to the particle trajectory (when $\Delta\psi$ at the entrance from the crystal equals $\Delta\psi$ at the exit), though generalization to an asymmetric case is straightforward. In fact, at practice such a generalization may be necessary even if the crystal is oriented symmetrically with respect to the beam axis, since non-negligible beam divergence compared to the crystal half-bending-angle makes the orientation asymmetric for individual particles [11].

A generic representation (valid at variable R and arbitrary orientation), which can be obtained based on the stationary phase approximation [2] ⁽⁴⁾, reads

$$(7) \quad \frac{dE_{\text{CBBC}}}{d\omega} = \int_{-L/2}^{L/2} dz \frac{dE_{\text{straight}}}{dz d\omega} \Big|_{\theta_x = |\xi'(z) - \theta_0|},$$

where $\xi(z)$ is the transverse coordinate of any of the bent atomic planes. If one utilizes here the known formula for the spectrum of coherent bremsstrahlung in a straight crystal (8)

$$\frac{dE_{\text{straight}}}{dz d\omega} = \frac{e^2 F_1^2 d^2}{2\pi^4 m^2 \theta_x^2} \frac{E'^2}{E^2} q_{\min} \sum_{n=1}^{\infty} \Theta \left(n - \frac{q_{\min}d}{2\pi|\theta_x|} \right) \frac{c_n^2}{n^{4+2\epsilon}} \left(1 - \frac{q_{\min}d}{n\pi|\theta_x|} + \frac{q_{\min}^2 d^2}{2n^2 \pi^2 \theta_x^2} + \frac{\omega^2}{2EE'} \right),$$

with $q_{\min}(\omega) = \frac{m^2 \omega}{2EE'}$, $E' = E - \omega$, $\theta_x(z) = \xi'(z) - \theta_0$, equation (7) turns to explicit Eq. (30) of paper [2]. To see the correspondence of Eqs. (6) and (7), one observes that in a uniformly bent crystal $\xi(z) = \frac{z^2}{2R} + \text{const}$, so integration variables $\theta_x = |z/R - \theta_0|$ and z are linearly related. In the ratio of $d\sigma^S \propto L$ and $\Delta\psi \propto \frac{L}{R}$ the crystal thickness L cancels out, so $\frac{dE}{d\omega} \propto R$. From the viewpoint of Eqs. (7, 8), the proportionality of the radiation spectrum to the crystal bending radius arises as

$$(9) \quad \frac{dE_{\text{CBBC}}}{d\omega} \propto \frac{dz}{dq} \sim Rd \sim l_{\text{EFC}}^2;$$

⁽⁴⁾ The replacement of Fresnel functions by step functions in [9] is equivalent to application of the stationary phase approximation in the original Fourier integrals.

see also Eq. (14) below.

For a uniformly bent crystal, further on, it is straightforward to accomplish integration over θ_x and arrive at Eq. (31) of [2], presenting the spectrum through a cubic polynomial function D . Averaging over angular distribution in the initial beam and account of multiple scattering in the crystal volume is also feasible analytically.

3.2. Coherence lengths and typical photon energies. – Evaluation of the spectrum of bremsstrahlung produced under a definite force $F(t)$ action on a charged particle often proceeds in two steps: (i) Fourier-decomposition of the external force, i.e., distinguishing virtual photons absorbed by the particle; (ii) conversion of the force spectrum to the radiation spectrum. An important physical scale characterizing each stage is its coherence length. In general, real photon emission (l_{form}) and virtual photon absorption (l_{EFC}) coherence lengths need not be related. Indeed, in simplest cases one has $l_{\text{EFC}} \rightarrow 0$ (stochastic scattering in an amorphous medium), or $l_{\text{EFC}} \rightarrow \infty$ (uniform external field), but $l_{\text{form}} = \frac{2EE'}{m^2\omega}$ always stays finite, providing for those cases the only coherence length to refer to. From the experience of the mentioned simplest cases, it had become common to call l_{form} simply ‘coherence length’, without specification of the nature of the coherence.

On the other hand, if the bremsstrahlung problem may be treated in the dipole approximation, the photon emission coherence is strictly related with the virtual photon absorption coherence: it reduces to Lorentz-rescaling of the frequency and integration of the intensity over typical $\sim \gamma^{-1}$ emission angles (cf. Eq. (11) below). Thence, it suffices to analyze the coherence in the external field Fourier decomposition.

In crystals, l_{EFC} acquires a finite size. In a straight crystal, this is just the distance between the planes crossed along the particle path; the irradiation resonance condition requires l_{form} to have the same value. Then,

$$(10) \quad l_{\text{form}} \sim l_{\text{EFC}} \simeq d/\theta_0 \quad (\text{straight crystal}).$$

At that, the typical radiation energy

$$(11) \quad \omega_0 \sim 2\gamma^2 l_{\text{form}}^{-1} \sim \gamma^2 \theta_0/d \quad (\text{straight crystal})$$

is just the Lorentz-rescaled plane-crossing frequency. The radiation spectral intensity is estimated as (cf. (8))

$$(12) \quad \frac{dE}{d\omega} = \frac{dE}{dzd\omega} L \propto \left(\frac{eF}{m}\right)^2 \frac{d^2}{\theta_0^2} \frac{L}{l_{\text{form}}(\omega)}, \quad l_{\text{form}}^{-1} = q_{\text{min}}(\omega) \lesssim \theta_0/d \quad (\text{straight crystal}).$$

Less trivial situation emerges in a bent crystal. There, the local frequency of plane crossing varies along the crystal, whereby there are 2 spatial scales:

$$(13) \quad l_{\text{EFC}} = \sqrt{2Rd} \quad (\text{bent crystal}),$$

on which the integrals from oscillatory gaussians ($\int dz e^{i\frac{z^2}{2Ra}} \dots$) converge, and the longitudinal geometrical scale of the crystal (say, its thickness L) determining the limiting frequency of plane crossing. If a tangency point of the particle trajectory with the family of bent planes occurs within the crystal, then

$$(14) \quad \frac{dE}{d\omega} \propto \left(\frac{eF}{m}\right)^2 l_{\text{EFC}}^2 \quad (\text{bent crystal}).$$

Comparing Eqs. (14) and (12), one sees that in both cases the radiation intensity is proportional to l_{EFC}^2 , which is in line with the understanding [10] of coherence length as the length at which radiation amplitudes add up. Besides that, (12) involves a factor $\frac{L}{l_{\text{form}}}$ arising due to spectral overlap of radiation generated within the crystal thickness in different coherence intervals (pile-up factor). In a bent crystal, where radiation from different coherence intervals does not overlap, factor $\frac{L}{l_{\text{EFC}}}$ enters the expression for the spectrum extent

$$(15) \quad \omega_{\text{end}} \propto \min \{4\pi\gamma^2 L / l_{\text{EFC}}^2, E\}$$

instead of intensity (14).

Since l_{EFC} and l_{form} appear to be important physical quantities, it is worth estimating their typical values. For $R \sim 20$ m, $d \approx 2$ Å, Eq. (13) gives $l_{\text{EFC}} \sim 100$ μm, whereas ratio $\frac{l_{\text{form}}}{l_{\text{EFC}}} \approx \frac{l_{\text{EFC}}}{L}$ is usually small (see Eq. (16) below). Therefore, without breaking the picture of CBBC, the crystal thickness may be decreased down to fractions of millimeter. Lastly, concerning the multiple scattering influence on the radiation, it is quantified by parameter $\frac{l_{\text{EFC}}}{l_{\text{mult}}}$, which is larger than LPM parameter $\frac{l_{\text{form}}}{l_{\text{mult}}}$, and therefore is more critical.

3.3. Locality of CBBC generation vs. straight crystal limit. – The observation that representation (6) contains a straight crystal limit may appear surprising from the viewpoint that local CBBC theory is based on the stationary phase approximation, whose condition assumes

$$(16) \quad l_{\text{EFC}} \ll L \quad (\text{CBBC locality condition}).$$

As R , and therewith l_{EFC} , increases, condition (16) must break down. Nevertheless, this does not destroy the convergence of the integral, provided

$$(17) \quad 4d/|\theta_0| \ll L \quad (\text{condition of many-interval crossing in a straight crystal}),$$

i. e., the particle crosses a large number of inter-planar intervals even in a straight crystal. If (17) holds, with the increase of R one sooner arrives at a condition

$$(18) \quad |\theta_0| \gg L/2R$$

than at (16). That implies that variation of the local plane-crossing frequency in the bent crystal is smaller than the frequency mean value, which is equivalent to near straightness of the crystal, regardless of whether condition (16) holds or not. In [2] it was demonstrated that under condition (18), Eqs. (7-8) indeed turn to the familiar formula of CBBC in a straight crystal, with the crystal bending radius dropping out. Hence, further increase of the radius will be inconsequential. The *linear*-exponent oscillatory integral convergence will be achieved at length (10) within the crystal thickness without the aid of crystal curvature. Together, conditions (16-17) may be cast into a universal expression for the convergence length: $l_{\text{conv}} = \min \{l_{\text{EFC}}, 4d/|\theta_0|\}$.

3.4. Radiation polarization. – For planar orientation of the crystal, when the particle is mainly subject to the force orthogonal to the active planes, there must be a significant

net polarization of the cone of emitted bremsstrahlung, directed orthogonally to the planes. According to [?], the polarization degree equals

$$(19) \quad P_{\text{net}}(\omega/E) = \frac{N^2}{2} \frac{1}{1 + \frac{3\omega^2}{4EE'}}$$

where the azimuthal anisotropy parameter N for planar orientation must be close to 1. Thereat, the maximal value of P_{net} is 50% at $\omega \ll E$, while at $\omega \rightarrow E$, $E' \rightarrow 0$, $P_{\text{net}} \rightarrow 0$.

4. – Conclusions

The problem of particle interaction with bent crystals in planar orientation contains many opportunities for analytic description. Some successes have already been achieved, linear laws of Fig. 4 being an example. Ultimately, for this class of problems there is a good perspective to calculate all the relevant observables without MC simulation, although the number of problems to deal with is large, and the goal remains remote presently.

* * *

The author wishes to Organizers of Channeling-2010 conference for local support. My special gratitude is to Prof. N.F. Shul'ga who introduced me to the subject of particle passage through matter when I was a student, and to Dr. A.V. Shchagin, who helped me keep in course of new experimental developments in this area.

REFERENCES

- [1] BONDARENCO M. V., *Phys. Rev. A*, **82** (2010) 042902.
- [2] BONDARENCO M. V., *Phys. Rev. A*, **81** (2010) 052903.
- [3] SCANDALE W. *et al.*, *Phys. Rev. Lett.*, **101** (2008) 234801.
- [4] TARATIN A. M. and VOROBIEV S. A., *Nucl. Instrum. Methods B*, **26** (1987) 512.
- [5] SHULGA N. F., TRUTEN' V. I., KIRILLIN I. V., *Talk given at Channeling-2010 Conference; www.lnf.infn.it/conference/channeling2010/presentations/101005/ch2010-shul'ga-1.pdf*
- [6] KOVALEV G. V., *JETP Lett.*, **87** (2008) 87; **87** (2008) 349; **89** (2008) 265.
- [7] MAISHEEV V. A., *Phys. Rev. ST Accel. Beams*, **10** (2007) 084701.
- [8] BABAEV A. and DABAGOV S. B., in: *Abstr. of Channeling-2010 Int. conf.*, (2010) p.105.
- [9] ARUTYUNOV V. A., KUDRYASHOV N. A., SAMCONOV V. M. and STRIKHANOV M. N., *Nucl. Phys. B*, **363** (1991) 283.
- [10] RYAZANOV M. I., *Sov. Phys. Usp.*, **17** (1975) 815.
- [11] BONDARENCO M. V., *J. Phys.: Conf. Ser.*, **236** (2010) 012026.